Check for updates

Received: 9 December 2021 | Accepted: 10 January 2022

DOI: 10.1111/gcb.16092

RESEARCH ARTICLE

Global Change Biology WILEY

High potential of stable carbon sequestration in phytoliths of China's grasslands

Zhaoliang Song[1] | Yuntao Wu[1] | Yuanhe Yang[2] | Xiaodong Zhang[1] | Lukas Van Zwieten[3] | Nanthi Bolan[4] | Zimin Li[5] | Hongyan Liu[6] | Qian Hao[1] | Changxun Yu[7] | Xiaole Sun[8] | Alin Song[9] | Wenying Wang[10] | Congqiang Liu[1] | Hailong Wang[11,12]

[1]School of Earth System Science, Institute of Surface-Earth System Science, Tianjin University, Tianjin, China

[2]State Key Laboratory of Vegetation and Environmental Change, Institute of Botany, Chinese Academy of Sciences, Beijing, China

[3]NSW Department of Primary Industries, Wollongbar, New South Wales, Australia

[4]School of Agriculture and Environment, Institute of Agriculture, University of Western Australia, Crawley, Western Australia, Australia

[5]Université catholique de Louvain (UCLouvain), Earth and Life Institute, Soil Science, Louvain-La-Neuve, Belgium

[6]College of Urban and Environmental Sciences, Peking University, Beijing, China

[7]Department of Biology and Environmental Science, Linnaeus University, Kalmar, Sweden

[8]Baltic Sea Center, Stockholm University, Stockholm, Sweden

[9]Key Laboratory of Crop Nutrition and Fertilization, Institute of Agricultural Resources and Regional Planning, Chinese Academy of Agricultural Sciences, Beijing, China

[10]Academy of Plateau Science and Sustainability, People's Government of Qinghai Province & Beijing Normal University, Qinghai, China

[11]School of Environment and Chemical Engineering, Foshan University, Guangdong, China

[12]Key Laboratory of Soil Contamination Bioremediation of Zhejiang Province, College of Environmental and Resource Sciences, Zhejiang A & F University, Zhejiang, China

Correspondence
Zhaoliang Song, School of Earth System Science, Tianjin University, No. 92 Weijin Road Nankai District, Tianjin 300072, China.
Email: zhaoliang.song@tju.edu.cn

Funding information
State's Key Project of Research and Development Plan of China, Grant/Award Number: 2016YFA0601002 and 2017YFC0212703; National Natural Science Foundation of China, Grant/Award Number: 41930862 and 42141014

Abstract

Phytolith carbon (C) sequestration plays a key role in mitigating global climate change at a centennial to millennial time scale. However, previous estimates of phytolith-occluded carbon (PhytOC) storage and potential in China's grasslands have large uncertainties mainly due to multiple data sources. This contributes to the uncertainty in predicting long-term C sequestration in terrestrial ecosystems using Earth System Models. In this study, we carried out an intensive field investigation (79 sites, 237 soil profiles [0–100 cm], and 61 vegetation assessments) to quantify PhytOC storage in China's grasslands and to better explore the biogeographical patterns and influencing factors. Generally, PhytOC production flux and soil PhytOC density in both the Tibetan Plateau and the Inner Mongolian Plateau had a decreasing trend from the Northeast to the Southwest. The aboveground PhytOC production rate in China's grassland was 0.48×10^6 t CO_2 a^{-1}, and the soil PhytOC storage was 383×10^6 t CO_2. About 45% of soil PhytOC was stored in the deep soil layers (50–100 cm), highlighting the importance of deep soil layers for C stock assessments. Importantly, the Tibetan Plateau had the greatest contribution (more than 70%) to the PhytOC storage in China's grasslands. The results of multiple regression analysis indicated that altitude and soil texture significantly influenced the spatial distribution of soil PhytOC,

 © 2022 John Wiley & Sons Ltd.

explaining 78.1% of the total variation. Soil phytolith turnover time in China's grasslands was mainly controlled by climatic conditions, with the turnover time on the Tibetan Plateau being significantly longer than that on the Inner Mongolian Plateau. Our results offer more accurate estimates of the potential for phytolith C sequestration from ecological restoration projects in degraded grassland ecosystems. These estimates are essential to parameterizing and validating global C models.

KEYWORDS
carbon sink, China's grasslands, ecological restoration, phytolith-occluded carbon, Tibetan Plateau, turnover time

1 | INTRODUCTION

Reducing atmospheric carbon dioxide (CO_2) emissions to mitigate global climate change is one of the biggest challenges for humanity (Fang et al., 2018; Hanssen et al., 2020). Being an important carbon (C) sink, the terrestrial ecosystem removes about 20–30% of the total anthropogenic CO_2 emissions (Tang et al., 2018). Biogeochemical C sequestration in terrestrial ecosystems, therefore, plays a significant role in mitigating global warming (Beaulieu et al., 2012; Parr & Sullivan, 2005; Parr et al., 2010; Song et al., 2012a, 2016). Previous studies on terrestrial C sequestration have been focused on the accumulation of biomass C and soil organic carbon (SOC) (Erb et al., 2018; Gherardi & Sala, 2020; Yao et al., 2018). However, as an important long-term stable C sequestration mechanism, the role of phytolith C sequestration in plants and soils has not been systematically studied at a national scale.

Plants absorb dissolved silicon (Si) from soil solution in the form of monosilicic acid (H_4SiO_4), transport it through the xylem via transpiration, and eventually deposit it in cell luminas, cell wall, and intercellular spaces to form phytoliths (Biru et al., 2021; Ma, 2003; Neumann, 2003; Piperno, 1988). Phytolith content (expressed as % dry matter) ranges from lower than 0.5% in most Dicotyledons to higher than 15% in some Poaceae (Parr et al., 2010; Song et al., 2016). This difference is mainly attributed to the environmental conditions and plant Si requirements (Guo et al., 2015; Hodson et al., 2005; Seyfferth et al., 2013). During phytolith formation, approximately 0.2–5.8% of organic C can be occluded within phytoliths to form phytolith-occluded carbon (PhytOC) (Parr & Sullivan, 2005; Parr et al., 2010), along with other elements and water (Li et al., 2014). When the plant material degrades or is burnt, phytoliths are released into soils. Some soils contain up to 3% of phytoliths, with the stable nature of PhytOC allowing C to be stored in soils or sediments across millennia (620–2100 years) (Parr & Sullivan, 2005; Wilding, 1967; Wilding et al., 1967). The abundance of phytoliths is highest in surface soils and decreases with soil depth (Blecker et al., 2006; Zhang et al., 2016a). The dissolution rate of phytoliths depends on soil type, climatic factors, and soil microbiological composition (Blecker et al., 2006; Song et al., 2016). The accumulation rate of soil PhytOC in terrestrial ecosystems is slow on an annual-decadal scale but could account for 15~37% of the global C sequestration rate at a centennial-millennial scale (Parr & Sullivan, 2005). The PhytOC storage in soil is 400–1000 times larger than the aboveground biomass in most terrestrial ecosystems (Blecker et al., 2006; Song et al., 2016), suggesting that PhytOC is a key long-term C sequestration mechanism and plays a crucial role in reducing atmospheric CO_2 concentrations.

Grasslands are widely distributed terrestrial ecosystems and play a crucial role in biogeochemical cycling of C and Si (Blecker et al., 2006; Song et al., 2016). Grasslands in China cover an area of approximately 4×10^8 ha, accounting for 41.7% of country's territory, and are mainly distributed in arid and semi-arid regions with various climatic conditions and altitude (Liu et al., 2018b). There is significant interest in the effects of climate change on the PhytOC production and accumulation in grasslands of China, especially on the Tibetan Plateau (Qi et al., 2016; Song et al., 2012b). The Tibetan Plateau is the largest plateau (about 2.0×10^6 km^2) on earth, and accommodates various alpine ecosystem types (Yang et al., 2008). The Inner Mongolian Plateau and the Tibetan Plateau have highly variable mean annual temperature (MAT), mean annual precipitation (MAP), and altitude. Previous studies have evaluated the PhytOC storages in different grassland ecosystems (e.g., Pan et al., 2017; Qi et al., 2016). However, these estimates cannot evaluate the current status of PhytOC storage in China's grasslands. Moreover, little is known about the impacts of various environmental conditions on phytolith and PhytOC densities in China's grasslands.

To fill these knowledge gaps, we undertook an intensive field sampling and analytical campaign to quantify phytoliths and PhytOC across the Inner Mongolian Plateau and the Tibetan Plateau. The main purposes of this study were to estimate the PhytOC storage in China's grasslands and to elucidate the possible anthropogenic and natural drivers of the spatial distributions of PhytOC storage to all the parameterization of global C models.

2 | MATERIALS AND METHODS

2.1 | Study area

This study assessed five major grassland types including temperate desert steppe (TDS), temperate typical steppe (TTS), temperate meadow steppe (TMS), alpine steppe (AS), and alpine meadow

(AM). The sites were located on the Inner Mongolian Plateau and Tibetan Plateau of China, extending 4500 km from the Northeast to the Southwest (Figure 1, Table 1). The growing season of vegetation is mainly from May to September, during which 80% of the annual precipitation occurs.

Grasslands of the Inner Mongolia Plateau include three steppes (i.e., TDS, TTS and TMS), which belong to the continental semi-arid grasslands of the Central Asian steppe ecosystem with a cold and dry mid-latitude climate (Kawamura et al., 2005; Wiesmeier et al., 2015). Meteorological data (1981–2010) shows a MAT from −2°C to 9°C, MAP of 152 to 502 mm, and mean annual evaporation covering from 1200 to 2500 mm (Dai et al., 2014). The altitude ranged from 185 to 2160 m. The TDS located in the west of the Inner Mongolia Plateau had Calcisol as the dominant soil type and the major community species were *Cleistogenes squarrosa*, *Agropyron mongolicum*, and *Carex duriuscula*. The TTS is located around the center of the Inner Mongolia Plateau, with Kastanozem as the dominant soil type and vegetation being *Stipa grandis*, *Stipa krylovii*, and *Artemisia sacrorum*. The TMS is located towards the east of the Inner Mongolia Plateau, with the dominant soil type being Chernozem, characterized as being very fertile with vegetation including *Stipa baicalensis*, *Filifolium sibiricum*, and *Carex pediformis* (Table 1) (Jin et al., 2018).

The native grasslands of the Tibetan Plateau are mainly covered by AS and AM, which accounts for more than 60% of the area in plateau (Yang et al., 2010). The region is characterized by cold weather with a MAT of −4 to 3°C, and low rainfall with an MAP of 295 to 518 mm, and an altitude ranging from 3174 to 4703 m, with an average of 4000 m. The dominant species were *Carex moorcroftii* and *Stipa purpurea* in AS, while *Kobresia humilis* and *Kobresia pygmaea* in AM (Ding et al., 2016). Based on the FAO soil taxonomy system, soil in both AS and AM was Cambisol (Yang et al., 2010).

2.2 | Field surveys and experimental analyses

This study selected a total of 79 sites including 20 sites on the Tibetan Plateau and 59 sites on the Inner Mongolia Plateau (Figure 1), representing a wide range of climatic conditions and altitudes. At each site, three soil profiles were excavated to the depth of 100 cm, and six soil layers were identified and sampled. Bulk density samples were obtained for each soil profile using the cutting ring method (100 cm^3 in volume). At the same location, 1 × 1 m quadrats with three replicates were randomly selected and the aboveground biomass was collected for calculating the aboveground net primary productivity (ANPP). After manually removing roots and stones, soil samples

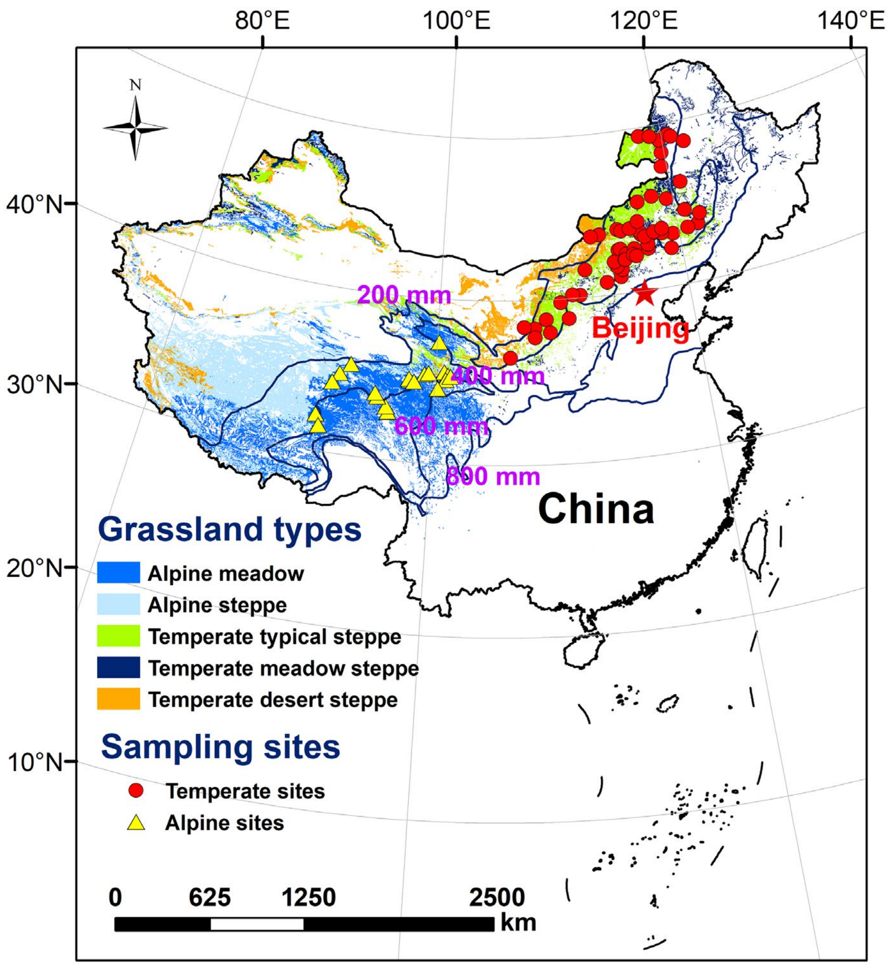

FIGURE 1 Distribution of sampling sites in China's grassland ecosystem

TABLE 1 Location, environment characteristics, and grassland type of each sampling site in China's grassland ecosystem

Sites	Longitude (°)	Latitude (°)	Altitude (m)	MAT (°C)	MAP (mm)	Grassland type
1	121.70	43.54	210	7.03	339.24	TDS
2	120.81	43.42	290	7.24	352.98	TDS
3	119.46	43.23	472	6.99	356.24	TDS
4	118.52	43.36	724	6.55	363.45	TDS
5	114.79	43.97	1126	2.54	243.33	TDS
6	115.10	43.85	1047	2.22	264.23	TDS
7	113.19	43.78	1026	4.07	178.86	TDS
8	112.48	43.70	915	4.57	152.50	TDS
9	115.03	42.19	1312	2.31	355.95	TDS
10	114.68	42.70	1159	3.42	282.95	TDS
11	114.86	42.75	1179	3.42	282.95	TDS
12	115.32	42.40	1265	2.31	355.95	TDS
13	108.42	38.79	1370	7.62	293.85	TDS
14	107.51	38.27	1297	7.78	291.41	TDS
15	106.68	38.36	1304	8.51	235.55	TDS
16	117.67	43.41	1191	3.25	394.42	TTS
17	117.27	43.21	1217	1.25	404.35	TTS
18	116.77	43.46	1276	1.51	369.30	TTS
19	116.64	43.70	1188	1.74	341.43	TTS
20	115.86	43.92	1102	2.44	280.89	TTS
21	116.62	44.29	1100	0.82	329.44	TTS
22	116.87	45.49	834	1.62	269.02	TTS
23	118.19	45.70	837	1.00	313.06	TTS
24	119.52	47.41	876	−2.28	434.58	TTS
25	119.75	48.26	880	−1.73	390.36	TTS
26	119.72	49.04	629	−0.88	349.16	TTS
27	114.69	41.06	1473	3.34	405.60	TTS
28	114.85	41.49	1400	3.34	405.60	TTS
29	114.45	41.70	1378	3.53	344.20	TTS
30	114.25	42.00	1464	3.22	301.57	TTS
31	115.17	42.07	1452	2.31	355.95	TTS
32	115.18	42.07	1398	2.31	355.95	TTS
33	116.04	42.66	1338	1.63	364.18	TTS
34	115.89	42.31	1381	2.32	367.13	TTS
35	116.15	42.20	1384	1.87	393.47	TTS
36	117.23	42.56	1544	1.20	428.77	TTS
37	117.23	42.81	1431	1.20	428.77	TTS
38	117.06	43.31	1269	1.25	404.35	TTS
39	117.88	43.52	940	1.92	392.15	TTS
40	118.58	43.64	907	4.86	377.80	TTS
41	120.81	44.52	297	5.91	380.02	TTS
42	122.03	44.15	185	6.69	344.04	TTS
43	119.13	42.34	573	7.93	386.46	TTS
44	113.49	40.81	1386	4.42	380.45	TTS

TABLE 1 (Continued)

Sites	Longitude (°)	Latitude (°)	Altitude (m)	MAT (°C)	MAP (mm)	Grassland type
45	111.77	41.71	1462	4.15	275.77	TTS
46	111.23	40.17	1047	7.69	391.69	TTS
47	110.62	40.23	992	8.03	370.77	TTS
48	109.62	39.80	1490	6.72	359.91	TTS
49	105.60	36.50	2160	8.33	301.08	TTS
50	107.50	37.71	1285	7.99	325.41	TTS
51	108.70	37.99	1250	8.26	379.34	TTS
52	110.22	38.79	1237	7.95	420.96	TTS
53	119.44	45.39	937	0.99	395.60	TMS
54	120.93	46.27	534	0.54	480.54	TMS
55	117.89	49.48	545	0.56	279.86	TMS
56	118.91	49.36	633	−0.55	310.52	TMS
57	120.63	49.29	650	−1.91	404.37	TMS
58	120.88	49.12	711	−1.91	404.37	TMS
59	122.01	48.69	620	−0.33	502.61	TMS
60	100.63	35.56	3304	1.73	399.67	AS
61	100.93	35.35	3174	1.35	406.35	AS
62	98.14	34.93	4242	−2.53	328.93	AS
63	98.07	35.01	4301	−3.58	409.53	AS
64	99.18	35.36	3225	−0.10	348.77	AS
65	93.67	35.49	4633	−1.27	232.73	AS
66	92.94	34.84	4593	−4.03	306.90	AS
67	92.49	34.27	4703	−3.30	295.87	AS
68	91.68	32.19	4532	−1.40	456.20	AS
69	100.77	35.08	3565	0.53	470.43	AM
70	101.12	35.3	3587	1.40	439.73	AM
71	100.22	34.52	3778	−0.13	507.00	AM
72	96.74	32.89	3958	3.27	518.43	AM
73	96.57	33.2	4289	0.70	493.87	AM
74	95.87	33.73	4161	−0.20	462.36	AM
75	95.7	33.95	4178	−0.90	436.07	AM
76	98.45	34.85	4165	−0.16	406.26	AM
77	99.48	35.44	3224	0.27	359.17	AM
78	100.13	37.36	3448	0.00	390.77	AM
79	91.99	31.54	4310	−0.40	456.00	AM

Abbreviations: AM, alpine meadow; AS, alpine steppe; MAP, mean annual precipitation; MAT, mean annual temperature; TDS, temperature desert steppe; TMS, temperature meadow steppe; TTS, temperature typical steppe.

Note: MAT and MAP in AS and AM are quoted from Ding et al. (2016).

were air-dried and sieved (2 mm) prior to further analysis. Soils from the bulk density rings from the Inner Mongolia Plateau were oven-dried for 24 h at 105°C to a constant weight for calculation of bulk density. The bulk density of soils from the Tibetan Plateau was calculated based on the empirical formula between soil organic matter and bulk density (Yang et al., 2007). Soil pH and EC were determined with a soil/water mass ratio of 1:5 using a pH/conductivity meter (Thermo, USA). The particle size distribution for soils from the Inner Mongolia Plateau samples was determined by a Laser Particle Sizer (Malvern Instruments Ltd., Worcestershire, United Kingdom), while those for soils from the Tibetan Plateau was taken from Fang et al. (2019). The SOC content was determined by combustion using an Elementar Analyzer (Vario EL III, Elementar, Germany) after removing soil inorganic C with hydrochloric acid (1 mol L^{-1}).

2.3 | Phytolith extraction in plants and soils

Phytoliths from the aboveground vegetation were extracted using a microwave digestion procedure (Parr & Sullivan, 2014). Phytoliths from soils were firstly wet oxidized by 30% H_2O_2 followed by a heavy liquid suspension ($ZnBr_2$, 2.36 g cm^{-3}) (Zuo et al., 2014). The phytoliths extracted from both plant and soil were digested using the Walkley-Black method to make sure that any organic matter outside the phytolith was completely removed (Parr & Sullivan, 2014; Walkley & Black, 1934). Thereafter, the extracted phytoliths were then oven-dried to a constant weight at 60°C for 48 h. The phytolith C content was measured by combustion using an Elementar Vario EL III. Quality assurance of methodologies was checked with a standard soil reference sample (GBW07405), and a precision better than 5% was obtained.

2.4 | Data analysis

In this study, PhytOC production fluxes of aboveground biomass were calculated based on the ANPP and plant PhytOC content as follows (Song et al., 2012b):

$$\text{PhytOC production flux} = \text{PhytOC content} \times \text{ANPP} \tag{1}$$

where PhytOC production flux is the PhytOC weight of aboveground biomass in per area per year (kg ha^{-2} yr^{-1}), PhytOC content is the PhytOC content in aboveground biomass (%), and ANPP is the aboveground net primary production of different grassland ecosystems (kg ha^{-2} yr^{-1}).

PhytOC production rate of different grassland ecosystems was calculated as follows:

$$\text{PhytOC production rate} = \text{PhytOC production flux} \times \text{area} \tag{2}$$

where PhytOC production rate is the total PhytOC production amount of aboveground biomass in different grassland ecosystems per year (10^6 t yr^{-1}), and the area is the total coverage of different grasslands in China (10^6 ha).

Soil PhytOC density in each grassland ecosystem was calculated as follows:

$$\text{Soil PhytOC density} = \sum_{i=1}^{n} \mathrm{T}_i \times \mathrm{BD}_i \times (\text{soil PhytOC content})_i \times \frac{(1 - \mathrm{C}_i)}{100} \tag{3}$$

where soil PhytOC density is the total amount of soil PhytOC per hectare in different grassland ecosystems (t ha^{-1}). T_i, BD_i, and C_i are the thickness (cm), bulk density (g cm^{-3}) and fraction percentage (>2 mm) at each soil layer i (i = 1, 2, 3…), respectively. Soil PhytOC content is the PhytOC content at soil layer i.

Soil PhytOC storage was calculated as follows:

$$\text{Soil PhytOC storage} = \text{soil PhytOC density} \times \text{area} \tag{4}$$

where soil PhytOC is the total amount of soil PhytOC in each grassland ecosystem (10^6 t). Soil PhytOC density was calculated by Equation (3) and area is the total coverage of each grassland ecosystem in China (10^6 ha).

In this study, assuming that the different grassland ecosystems were at steady state and all phytolith production per area per year would be returned to the soil profile via litter decomposition. We calculated soil phytolith turnover time at a national scale based on soil phytolith pool and phytolith return flux. Thus, soil phytolith turnover times in the different grassland ecosystems were calculated as follows (Blecker et al., 2006):

$$\text{Soil phytolith turnover time} = \frac{\text{soil phytolith density}}{\text{phytolith production flux}} \tag{5}$$

where the units of soil phytolith turnover, soil phytolith density and phytolith production flux are year, t ha^{-1} and t ha^{-1} a^{-1}, respectively.

After the normality tests, least square difference and one-way analysis of variance were used to evaluate whether the soil PhytOC distribution significantly differed among the various grassland ecosystems. Pearson correlation coefficients were performed to reveal the correlations between density or storage of soil PhytOC and environment variables (e.g., MAT, MAP, pH, clay, silt). In addition, stepwise multiple linear regression was performed to assess the variance in soil PhytOC explained by soil physicochemical properties and climatic factors.

3 | RESULTS

3.1 | Distribution of PhytOC across grasslands

The phytolith content of aboveground vegetation varied significantly ($p < .05$) and ranged from 2.6% to 5.8% across different grassland ecosystems (Table 2). Generally, phytolith content was the highest in the AS (5.8 ± 4.2%), followed by TMS (4.1 ± 1.7%), TDS (4.2 ± 2.6%), AM (3.2 ± 1.5%), and TTS (2.6 ± 1.3%). The PhytOC content of aboveground vegetation across different grasslands ranged from 0.0468 to 0.0738%, with no significant difference among different grassland types (Table 2).

Soil phytolith and PhytOC densities exhibited a large spatial variability across the Inner Mongolia Plateau and Tibetan Plateau and generally decreased from the Northeast to the Southwest. On the Inner Mongolia Plateau, soil PhytOC density decreased from 0.43 ± 0.01 t ha^{-1} in the TMS to 0.26 ± 0.02 t ha^{-1} in the TDS. On the Tibetan Plateau, soil PhytOC density decreased from 0.76 ± 0.07 t ha^{-1} in the AM to 0.56 ± 0.06 t ha^{-1} in the AS (Table 3). The densities of soil phytolith and PhytOC in different grassland ecosystems decreased in the order of AM > AS > TMS > TTS > TDS (Figure 2). In addition, soil phytolith and PhytOC in soil profiles of different grassland ecosystems displayed a similar vertical distribution pattern, decreasing with increasing soil depth (to 100 cm). The proportion of soil PhytOC in the top 50 cm averaged 55.2 ± 1.7% (Figure 3).

TABLE 2 PhytOC production fluxes and rates in different grassland ecosystems

Grassland type	Phytolith content (%)	PhytOC content in plant (%)	ANPP[a] (kg ha^{-1})	Area[b] (10^6 ha)	PhytOC production flux (kg ha^{-1} yr^{-1})	PhytOC production rate (10^6 t yr^{-1})
TDS	4.19 ± 2.63	0.0681 ± 0.0490	608.6	18.31	0.415 ± 0.298	0.0076 ± 0.0055
TTS	2.58 ± 1.29	0.0495 ± 0.0326	1671.4	38.52	0.827 ± 0.545	0.0319 ± 0.0210
TMS	4.06 ± 1.73	0.0610 ± 0.0251	2887.3	7.64	1.762 ± 0.725	0.0135 ± 0.0055
AS	5.78 ± 4.22	0.0738 ± 0.0570	677.0	70.81	0.499 ± 0.386	0.0354 ± 0.0273
AM	3.15 ± 1.46	0.0468 ± 0.0269	1559.0	58.73	0.730 ± 0.419	0.0429 ± 0.0246
Total/average					0.847 ± 0.475	0.1311 ± 0.0839

Abbreviations: AM, alpine meadow; AS, alpine steppe; TDS, temperate desert steppe; TMS, temperate meadow steppe; TTS, temperate typical steppe.

[a] ANPP, aboveground net primary productivities in different grasslands are quoted from Hu et al. (2006) and Shen et al. (2016).

[b] Area, the area of different grasslands are quoted from Ma et al. (2010).

TABLE 3 Densities of soil SOC, phytolith and PhytOC, and soil PhytOC storages in different grassland ecosystems

Grassland Type	SOC density (t ha^{-1})	Phytolith density (t ha^{-1})	PhytOC density (t ha^{-1})	PhytOC storage (10^6 t)
TDS	46.88	33.87 ± 2.78	0.26 ± 0.02	4.78 ± 0.39
TTS	97.28	33.75 ± 3.5	0.31 ± 0.03	11.88 ± 1.15
TMS	172.11	57.33 ± 2.08	0.43 ± 0.01	3.27 ± 0.10
AS	57.32	81.06 ± 5.51	0.56 ± 0.06	39.98 ± 3.90
AM	127.25	90.57 ± 4.64	0.76 ± 0.07	44.73 ± 4.02
Total/average			0.46 ± 0.04	104.65 ± 9.57

Abbreviations: AM, alpine meadow; AS, alpine steppe; TDS, temperate desert steppe; TMS, temperate meadow steppe; TTS, temperate typical steppe; SOC, soil organic carbon.

Note: Soil depth is 100 cm.

3.2 | Production and storage of PhytOC in different grasslands

The estimated production fluxes and accumulation rates of PhytOC in different grassland ecosystems varied significantly (Table 2, Figure 4b). PhytOC production flux was the highest in the TMS (1.76 ± 0.73 kg ha^{-1} yr^{-1}), followed by the TTS (0.83 ± 0.55 kg ha^{-1} yr^{-1}), AM (0.73 ± 0.42 kg ha^{-1} yr^{-1}), AS (0.50 ± 0.39 kg ha^{-1} yr^{-1}), and TDS (0.42 ± 0.30 kg ha^{-1} yr^{-1}). However, PhytOC production rate was highest in the AM (0.043 ± 0.025 × 10^6 t yr^{-1}), followed by the AS (0.035 ± 0.027 × 10^6 t yr^{-1}) and TTS (0.032 ± 0.021 × 10^6 t yr^{-1}), and lowest in TMS (0.014 ± 0.006 × 10^6 t yr^{-1}) and TDS (0.008 ± 0.006 × 10^6 t yr^{-1}).

Estimated soil PhytOC storage varied greatly among different grassland ecosystems at the national scale (Table 3). The soil PhytOC stored within the top 100 cm soil layers of the TDS, TTS, TMS, AS, and AM was calculated to be 4.8 ± 0.4, 11.9 ± 1.2, 3.3 ± 0.1, 40.0 ± 3.9, and 44.7 ± 4.0 × 10^6 t, respectively. The 0–100 cm soil layer of different grassland ecosystems in China stored a total of 104.7 ± 9.6 × 10^6 t PhytOC and displayed significantly different capacities to store PhytOC ($p < .05$) (Figure 4a).

3.3 | Turnover times of soil phytoliths in different grasslands

Phytolith turnover times calculated for the top soil layers (0–100 cm) displayed a great spatial variability ($p < .05$), ranging from 489 ± 42 years to 2072 ± 193 years (Figure 5). The longest turnover time was found on the Tibetan Plateau, where the turnover time was significantly longer than that on the Inner Mongolia Plateau. The turnover time for soil phytoliths on the Inner Mongolia Plateau was in the order of TDS > TTS > TMS. No significant difference was observed between the AM and AS (Figure 5).

4 | DISCUSSION

4.1 | Factors controlling the PhytOC in China's grasslands

The national field survey provided a comprehensive data set of PhytOC distribution in China's grasslands. Both the aboveground PhytOC production fluxes and soil PhytOC densities showed a

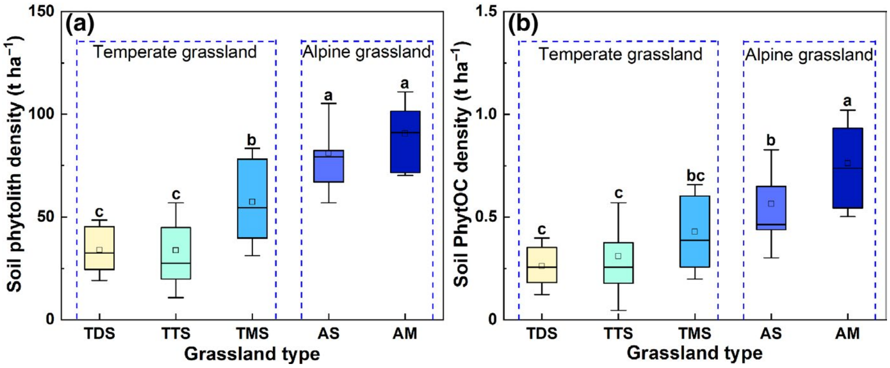

FIGURE 2 The densities of soil phytolith and PhytOC in different grassland ecosystems (soil depth is 100 cm)

significant difference among the grassland ecosystems ($p < .05$) (Tables 2 and 3). Aboveground PhytOC production flux in the TMS was the highest among all grassland ecosystems. This large difference may be linked to several factors including the variation in ANPP. For example, based on the remote sensing data set of the vegetation index between 1982 and 2011 and supporting field measurements, ANPP varied broadly from 610 to 28,900 kg·ha^{-2}·yr^{-1} (Hu et al., 2006; Shen et al., 2016). Annual variation of grassland ANPP showed a clear fluctuation among the different regions. The availability of soil nutrients played a significant role in controlling vegetative growth and ANPP (Fay et al., 2015). The plant composition and diversity were also influenced by precipitation and temperature (Jin et al., 2013; Shimono et al., 2010; Tang et al., 2012). As reported by Shen et al. (2016), the species richness decreased in the order of TMS (19) > AM (18) > TTS (11) > AS (9) > TDS (8). The contents of phytoliths in different plant species ranged from less than 0.5% (Dicotyledons) to more than 15% (Poaceae) (Epstein, 1994; Parr et al., 2010), which was mainly influenced by plant phylogeny (Ji et al., 2018) and bioavailability of soil Si (Hodson et al., 2005; Song et al., 2016). Ji et al. (2018) analyzed the Si contents of 184 plant species in grasslands of Northern China and found that the Si contents of aboveground biomass ranged from 2.15 to 6.53 g kg^{-1}. In addition, previous studies revealed that the addition of Si-rich fertilizers to agricultural systems could increase soil Si availability, thereby enhancing the phytolith content with the concomitant increase in Si uptake by rice or wheat (Guo et al., 2015; Meena et al., 2014; Tombeur et al., 2021). The different PhytOC contents among various grassland ecosystems could also be influenced by the carbohydrate content of plant cell walls, which can increase the phytolith content of plant tissues (Hodson, 2016). Consequently, ANPP, plant species composition, soil Si availability and PhytOC/phytolith content of aboveground biomass interact with each other and eventually lead to the current distribution status of PhytOC production fluxes in grassland ecosystems.

Soil phytolith and PhytOC contents were generally the greatest in the topsoil (usually in the A-horizon) and decreased with increasing soil depth. This phenomenon was in agreement with previous results for forest (Zhang et al., 2016a), wetland (Li et al., 2013), and other grassland studies (Pan et al., 2017). These findings suggest that the distribution of soil phytoliths and PhytOC is

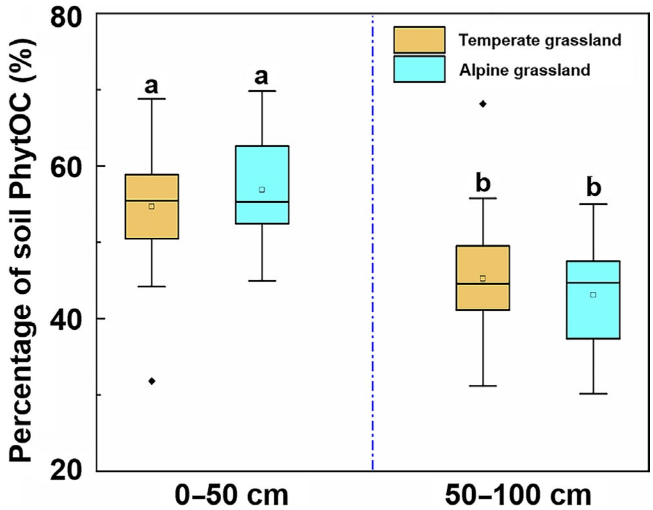

FIGURE 3 The percentage of soil PhytOC in different soil layers in China's grassland

controlled by aboveground inputs, migration and dissolution followed by microbial degradation in the soil profile (Blecker et al., 2006; Fishkis et al., 2009). In addition, our results indicated that soil PhytOC density on the Tibetan Plateau was significantly higher than that on the Inner Mongolia Plateau (Table 3, Figure 6), which was mainly due to the environmental differences (e.g., MAT; MAP and altitude) between the two plateaus. It should be noted that soil PhytOC densities on the Inner Mongolia Plateau and Tibetan Plateau generally decreased from the Northeast to the Southwest. All these distribution trends are influenced by the ANPP, climatic factors and soil physicochemical properties. The soil PhytOC density increased with increasing aboveground PhytOC production fluxes in both the Tibetan Plateau and Inner Mongolia Plateau (Figure 6), indicating that ANPP and aboveground phytolith content play a key role in regulating soil PhytOC density (Li et al., 2013; Zhang et al., 2016a). Climate has been shown to be an important influencing factor for soil PhytOC density (Blecker et al., 2006; Zhang et al., 2020). Our data showed that soil PhytOC density was negatively correlated with MAT, but positively with MAP (Figure 7). Increasing temperature could enhance the decomposition of soil phytoliths by stimulating soil microbial activity (Song et al., 2016; Yang et al., 2008). However, precipitation leads

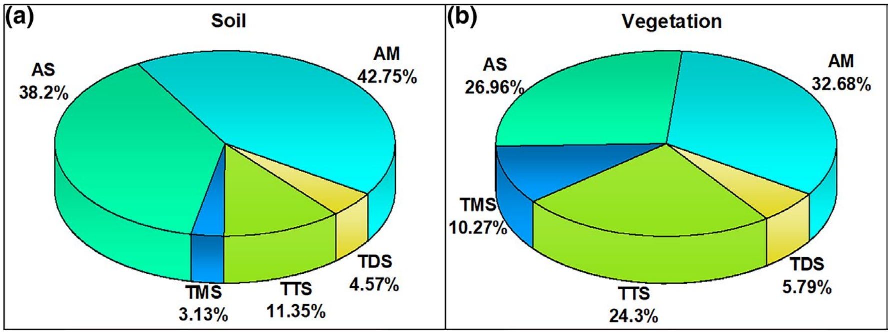

FIGURE 4 The percentages of soil PhytOC storage and PhytOC production rate in different grassland ecosystems

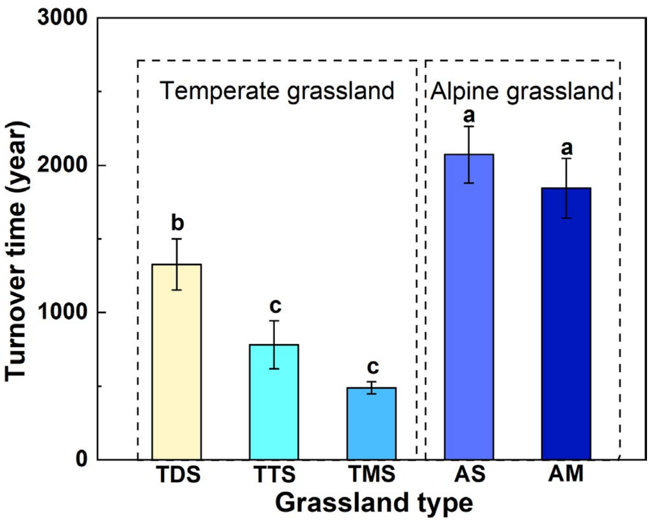

FIGURE 5 Soil phytolith turnover times in different grassland ecosystems

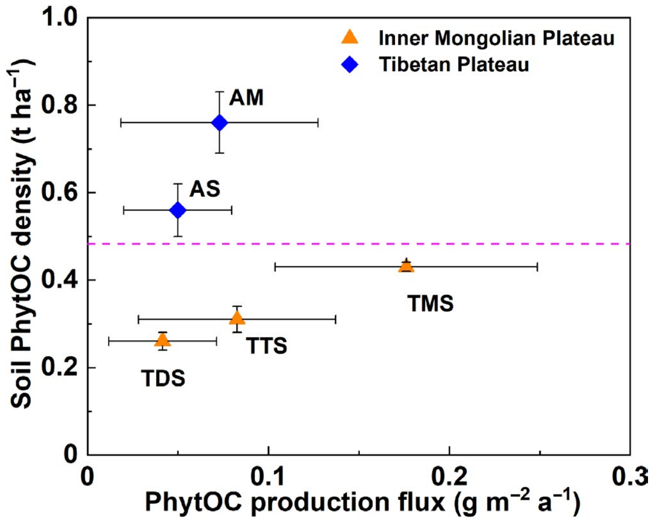

FIGURE 6 Relationship between PhytOC production flux and soil PhytOC density

to increasing availability of soil water, increasing NPP (Bai et al., 2008; Wynn et al., 2006), and positively influencing PhytOC production and consequently density of PhytOC in soil.

Soil PhytOC densities in both the Inner Mongolia Plateau and Tibetan Plateau were significantly different (Inner Mongolia Plateau: TMS > TTS > TDS; Tibetan Plateau: AM > AS) (Table 3). These differences are due to the differences in production inputs, and migration, dissolution and microbial degradation. The aboveground PhytOC production fluxes of TTS and TMS on the Inner Mongolia Plateau were significantly higher than that on the Tibetan Plateau, however, the average soil PhytOC density on the Tibetan Plateau was greater than that in Inner Mongolia Plateau (0.66 vs. 0.33 t ha^{-1}). We suggest that the large difference in altitude between the two plateau regions could influence this, along with the differences in temperature and precipitation. For example, the average altitude of the Tibetan Plateau region (4239 m) is significantly higher than that of the Inner Mongolian Plateau region (1066 m), resulting in a lower MAT on the Tibetan Plateau compared to the Inner Mongolia Plateau (−1 vs. 2°C) (Ma et al., 2012). In addition, due to the high altitude, the Tibetan Plateau has a large area of permafrost (about 1.35×10^8 ha), which covers about 67% of the plateau area (Ding et al., 2016; Mu et al., 2015). The low-temperature conditions of permafrost would result in lower microbial decomposition rates thus limiting soil PhytOC mineralization. Of the variables examined, altitude explained the largest proportion (~57.9%) of the total variation of soil PhytOC density and is, thus, the primary factor influencing the distribution of soil PhyOC in China's grassland ecosystem.

Soil physicochemical properties can also largely influence soil phytolith and PhytOC densities (Bartoli, 1985; Cornelis et al., 2011; Farmer et al., 2005; Fraysse et al., 2006). For example, increasing soil silt and clay contents could suppress microbial activity (Nguyen et al., 2019; Schimel et al., 1994; Torn et al., 1997; Wynn et al., 2006), facilitating the preservation of soil phytolith and PhytOC. Li et al. (2020) reported that 60% of the soil phytoliths occurred within soil macroaggregates, supporting the notion that soil aggregation protects phytoliths from microbial decomposition and rapid dissolution. Our data support these results which showed that soil phytolith and PhytOC density were positively correlated with soil clay content, explaining 17.9% of the spatial variation (Table 4). The soil pH buffering capacity largely drives the phytolith dissolution rate (Li et al., 2019; Song et al., 2016), affecting its storage and PhytOC density (Figure 7). In addition, the availability of soil metal ions (e.g., Fe^{3+}, Al^{3+}) in soils, although not analyzed by this study, could also influence the dissolution rate of soil phytoliths because of their high ability to complex and thus stabilize soil phytoliths (Bartoli & Wilding, 1980; Dan & Ruth, 2015; Nguyen et al., 2014).

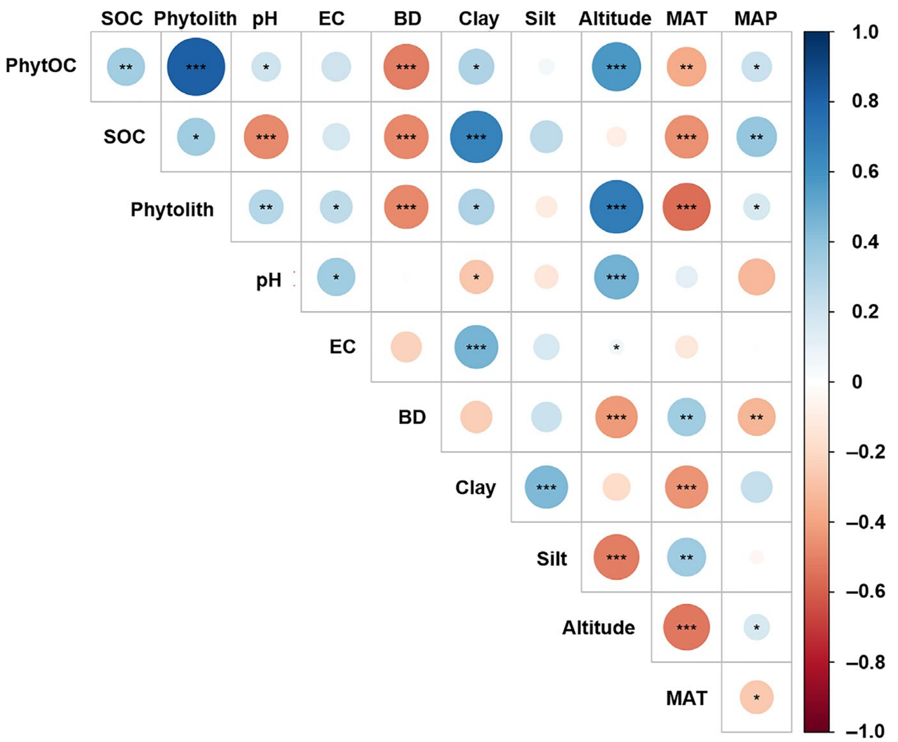

FIGURE 7 The correlations between soil PhytOC storage and environmental and edaphic factors

TABLE 4 Results of the multiple regressions refer to the final accepted model, which just included the effects of the significant variables for PhytOC density in China's grassland

	Unstandardized coefficients		Standardized coefficients		
Variables	*B*	SE	Beta	t	Sig.
Constant	0.500	0.284		1.762	0.084
Altitude	0.000	0.000	0.705	6.553	0.000
Clay	0.014	0.007	0.215	2.053	0.045
Silt	0.003	0.001	0.368	3.314	0.002
BD	−0.384	0.173	−0.229	−2.216	0.031

4.2 | Effects of climate on soil phytolith turnover

Phytolith-occluded C can be preserved in soils or sediments for hundreds to thousands of years (Blecker et al., 2006; Meunier & Fabrice, 1999; Parr & Sullivan, 2005; Song et al., 2012a). It should be noted that phytoliths in different soil layers are dissolved at various rate and it is impossible to examine the actual dynamics of each soil phytolith due to their high abundance (Alexandre et al., 1997; Song et al., 2016). Thus, as the dissolution rate of phytolith varies, the estimation of average turnover time of phytolith in soil profiles is commonly used to calculate soil PhytOC storage capacity.

The average turnover times of soil phytoliths on the Inner Mongolia Plateau showed significant differences ($p < .05$) among the studied grassland ecosystems: TDS (1327 ± 173 years) > TTS (782 ± 162 years) > TMS (488 ± 41 years) (Figure 5). This difference was mainly attributed to MAP. On the Inner Mongolia Plateau, there was no significant difference in the MAT among various grassland ecosystems, while soil phytolith turnover times decreased with increasing MAP (ranging from 200 to 500 mm). This finding was consistent with the results of Blecker et al. (2006). These results further suggest that high soil water availability simultaneously promotes both ANPP and soil phytolith dissolution, resulting in a higher turnover rate of soil phytoliths. However, MAT in AM and AS are similar and MAP in AM is generally higher than that in AS (442 vs. 346 mm). The average turnover times of soil phytoliths in AM and AS were similar (1844 vs. 2072 years), suggesting that MAT (as opposed to MAP) was the main factor controlling the turnover time of soil phytoliths on the Tibetan Plateau. We found that the average turnover time of soil phytoliths on the Inner Mongolia Plateau (866 ± 126 years) was significantly shorter than that in Tibetan Plateau (1958 ± 198 years). This difference may be attributed to the lower MAT and higher altitude in Tibetan Plateau leading to lower decomposition rate compared to the Inner Mongolia Plateau (–1 vs. 2°C, 4239 vs. 1066 m).

In this study, the turnover time of soil phytoliths estimated by our might have some biases. Firstly, we assumed that all grassland ecosystems were at a steady state. In reality, few soil profiles could be maintained in a long-term steady state due to climate variability as well as anthropogenic and natural disturbance (e.g., land-use change and fire) (Yan et al., 2017). Previous studies have indicated that permafrost in Tibetan Plateau has experienced pronounced warming and is thawing gradually over the last decades, which may lead to nutrient release (e.g., nitrogen and phosphorus) (Ding et al., 2016; Schuur et al., 2015). Only if the disturbance and climate fluctuations are regular, the soil profiles can be considered to be in quasi-steady state (Luo et al., 2019). Secondly, we did not take into account the spatial variability of soil properties in different grassland ecosystems. Although our results suggest that climate plays the dominant role in controlling soil phytolith turnover time, previous studies have indicated that soil properties exerted the most important influences on SOC turnover, especially in subsoils (Luo et al., 2019). Hence, comprehensive studies on the effect of soil properties and climate on soil phytolith turnover should be strengthened in the future. Thirdly, the turnover times of soil phytoliths can vary greatly with soil depth. Phytoliths in deep soils are more stable compared to those in the topsoil (Parr & Sullivan, 2005), potentially influencing our results. This may lead to the underestimation of phytolith turnover time. We acknowledge that more accurate estimates of soil phytolith turnover time and controlling factors may be achieved once these aforementioned gaps in knowledge are addressed.

4.3 | Potential of phytolith C sequestration in terrestrial ecosystems

This study provides a regional-scale and comprehensive investigation of PhytOC storage in China's grassland ecosystem. The aboveground PhytOC production rate in China's grasslands is equivalent to about 0.48×10^6 t CO_2 yr^{-1}, approximately 60% of which comes from the grassland on the Tibetan Plateau. The rate was similar to the previous estimation for the grasslands in China (0.6×10^6 t CO_2 yr^{-1}) (Song et al., 2012b) but lower than that of North American grasslands (1.0×10^6 t CO_2 yr^{-1}) (Blecker et al., 2006). Because ANPP plays a key role in determining the aboveground PhytOC production rate, the difference is mainly attributed to the lower ANPP in China's grasslands compared to North American grasslands (940–4240 kg ha^{-1}). It should be noted that Shen et al. (2016) found that the average above- and belowground biomass density of China's grasslands in the past 30 years (1982–2011) was 1780 and 7590 kg ha^{-1}, respectively, showing that the belowground biomass density was about 4.3 times higher than that of the aboveground (Shen et al., 2016). This also highlights the role of the belowground PhytOC production rate in long-term C sequestration and should be taken into account in C budgets in global terrestrial systems in the future.

The grasslands on the Tibetan Plateau store more than 70% of the PhytOC in the top 100 cm soil layer across China's grasslands (383×10^6 t CO_2), suggesting that the Tibetan Plateau plays an important role in long-term C sequestration in China. It should be noted that the proportion of PhytOC to SOC increases with soil depth, especially in AM, and about 45% of soil PhytOC occurred in deep layers (50–100 cm) (Figure 3). Therefore, deep soil PhytOC should be included in the assessment of soil PhytOC storage of grassland ecosystems. The soil thickness in some grassland ecosystems could reach several meters (e.g., TMS and AM steppe). Ding et al. (2016) evaluated the storage and spatial variation of SOC down to 300 cm depth in Tibetan Plateau and found 44% of SOC occurred in deeper layers (e.g., 100–300 cm). Therefore, understanding processes and storage capacity below 100 cm may be important to better estimate C storage potential.

China's grasslands serve as important green barriers for national ecological security. However, due to enhanced human disturbance and climate change (Jiang et al., 2006), almost all of China's grasslands are affected by some form of degradation, leading to deterioration of soil C storage (Pan et al., 2017). Since the late 1970s, a series of ecological restoration projects have been carried out in China to restore degraded ecosystems (e.g., Returning Grazing Land to Grassland Project and Beijing-Tianjin Sand Source Control Project), covering about one quarter of China's grasslands (Lu et al., 2018). These projects have substantially increased C stock in specific regions, especially in the north of China. For example, Deng et al. (2017) found that large scale grazing exclusion has promoted grassland C sequestration. Given the positive correlation between SOC and soil PhytOC (Figure 7), we suggest that decreasing grazing intensity has a high potential to increase the aboveground PhytOC production rate and soil PhytOC storage in China's grassland ecosystems, especially in degraded semi-arid grassland ecosystems. Meanwhile, Zhao et al. (2015) found that nitrogen fertilizer application could effectively increase the PhytOC production flux in the extremely degraded grassland, which indicates that the optimization of nutritional application is a promising approach to increase phytolith C sequestration in degraded grassland ecosystem. Besides, increasing the proportion of Poaceae and Cyperaceae during grassland management can further increase PhytOC production flux and rate (Song et al., 2012b).

Importantly, China's grasslands have experienced significant warming in the past 50 years and this warming trend will further intensify in the future (Liu et al., 2018a; Zhang et al., 2016b). Climate change can have significant impacts on plant species composition, NPP and temperature sensitivity of SOC, especially in high-altitude permafrost regions like the Tibetan Plateau. For example, Liu et al. (2018a) found that the changes to plant species composition in Tibetan Plateau in response to climate change have shifted from aboveground to belowground productivity. It is clear that PhytOC production rate and soil PhytOC storage in China's grassland ecosystems is experiencing a dramatic and dynamic change. Future studies should be combined with biogeochemical models, which will provide valuable data sets for the estimation of C turnover and storage potential in terrestrial ecosystems.

To sum up, this study indicated that there were significant differences in the aboveground PhytOC production fluxes and soil PhytOC density among various grassland ecosystems, due to the variations of climate, soil physicochemical properties and human disturbance. The aboveground PhytOC production rate and soil

PhytOC storage (~100 cm) in China's grasslands were 0.48×10^6 and 383×10^6 t CO_2, respectively, more than 70% of which were on the Tibetan Plateau. Most importantly, soil phytolith turnover time on the Tibetan Plateau was significantly longer than that on the Inner Mongolian Plateau, reinforcing the importance of the Tibetan Plateau for long-term C storage. Moreover, Lu et al. (2018) noted that the total C sequestration rate in China's grasslands was 0.26 Mg C ha^{-1} yr^{-1} between 2001 and 2010 due to national ecological restoration projects, which reinforces the significant potential of grasslands to be a PhytOC sink. Our findings also indicate that management measures (e.g., organic mulching and silicon fertilization in croplands; bamboo afforestation/reforestation) to maximize net primary production and plant phytolith content can effectively increase phytolith C sequestration in other terrestrial ecosystems. Further studies should focus on the assessment of deep soil PhytOC dynamics in China's grassland ecosystems and the development of models that can better predict storage potential based on land management practices. Technologies that can monitor and model the spatial distribution and dynamic change of soil phytoliths on both the national and global scales will improve estimates of soil PhytOC storage. Our data also have provided a comprehensive and unique data set for studying the coupled terrestrial biogeochemical cycles of Si and C.

ACKNOWLEDGEMENTS

The research was supported by the National Natural Science Foundation of China (41930862 and 42141014), State's Key Project of Research and Development Plan of China (2016YFA0601002 and 2017YFC0212703).

CONFLICT OF INTEREST

The authors declare that they have no known competing financial interests or personal relationships that could have appeared to influence the work reported in this paper.

AUTHOR CONTRIBUTION

Z. Song designed the study. Z. Song and Y. Wu performed the analysis. Z. Song, Y. Wu, and X. Zhang prepared figures and drafted the paper. Y. Yang, Z. Li, H. Liu, Q. Hao, C. Yu, X. Sun, A. Song, L.Z., N.B., W. Wang, C. Liu, and H. Wang contributed to the interpretation of the results and provided critical revision of the article. All authors provided final approval of the revision to be published.

DATA AVAILABILITY STATEMENT

The data that support the findings of this study are openly available in figshare at http://doi.org/10.6084/m9.figshare.18585983.

ORCID

Zhaoliang Song https://orcid.org/0000-0002-2219-5852
Yuanhe Yang https://orcid.org/0000-0002-5399-4606
Zimin Li https://orcid.org/0000-0002-6377-2636
Hongyan Liu https://orcid.org/0000-0002-6721-4439
Changxun Yu https://orcid.org/0000-0002-0635-3718

REFERENCES

Alexandre, A., Meunier, J. D., Colin, F., & Koud, J. M. (1997). Plant impact on the biogeochemical cycle of silicon and related weathering processes. *Geochimica Et Cosmochimica Acta*, *61*(3), 677–682. https://doi.org/10.1016/S0016-7037(97)00001-X

Bai, Y. F., Wu, J. G., Xing, Q., Pan, Q. M., Huang, J. H., Yang, D. L., & Han, X. G. (2008). Primary production and rain use efficiency across a precipitation gradient on the mongolia plateau. *Ecology*, *89*(8), 2140–2153. https://doi.org/10.1890/07-0992.1

Bartoli, F. (1985). Crystallochemistry and surface properties of biogenic opal. *Journal of Soil Science*, *36*(3), 335–350. https://doi.org/10.1111/j.1365-2389.1985.tb00340.x

Bartoli, F., & Wilding, L. P. (1980). Dissolution of biogenic opal as a function of its physical and chemical properties. *Soil Science Society of America Journal*, *44*(4), 873–878. https://doi.org/10.2136/sssaj1980.03615995004400040043x

Beaulieu, E., Godderis, Y., Donnadieu, Y., Labat, D., & Roelandt, C. (2012). High sensitivity of the continental-weathering carbon dioxide sink to future climate change. *Nature Climate Change*, *2*(5), 346–349. https://doi.org/10.1038/nclimate1419

Biru, F. N., Islam, T., Cibils-Stewart, X., & Cazzonelli, C. I. (2021). Anti-herbivore silicon defences in a model grass are greatest under miocene levels of atmospheric CO_2. *Global Change Biology*, *27*(10), 2959–2969. https://doi.org/10.1111/gcb.15619

Blecker, S. W., McCulley, R. L., Chadwick, O. A., & Kelly, E. F. (2006). Biologic cycling of silica across a grassland bioclimosequence. *Global Biogeochemical Cycles*, *20*(3). https://doi.org/10.1029/2006GB002690

Cornelis, J. T., Delvaux, B., Georg, R. B., Lucas, Y., Ranger, J., & Opfergelt, S. (2011). Tracing the origin of dissolved silicon transferred from various soil-plant systems towards rivers: A review. *Biogeosciences*, *8*(1), 89–112. https://doi.org/10.5194/bg-8-89-2011

Dai, E. F., Zhai, R. X., Ge, Q. S., & Wu, X. Q. (2014). Detecting the storage and change on topsoil organic carbon in grasslands of Inner Mongolia from 1980s to 2010s. *Journal of Geographical Sciences*, *24*(6), 1035–1046. https://doi.org/10.1007/s11442-014-1136-9

Dan, C., & Ruth, S. G. (2015). Understanding fossil phytolith preservation: The role of partial dissolution in paleoecology and archaeology. *PLoS One*, *10*(5), e0125532. https://doi.org/10.1371/journal.pone.0125532

Deng, L., Shangguan, Z. P., Wu, G. L., & Chang, X. F. (2017). Effects of grazing exclusion on carbon sequestration in China's grassland. *Earth-Science Reviews*, *173*, 84–95. https://doi.org/10.1016/j.earscirev.2017.08.008

Ding, J. Z., Li, F., Yang, G. B., Chen, L. Y., Zhang, B. B., Liu, L., Fang, K., Qin, S. Q., Chen, Y. L., Peng, Y. F., Ji, C. J., He, H. L., Smith, P., & Yang, Y. H. (2016). The permafrost carbon inventory on the Tibetan Plateau: A new evaluation using deep sediment cores. *Global Change Biology*, *22*(8), 2688–2701. https://doi.org/10.1111/gcb.13257

Epstein, E. (1994). The anomaly of silicon in plant biology. *Proceedings of the National Academy of Sciences*, *91*(1), 11–17. https://doi.org/10.1073/pnas.91.1.11

Erb, K. H., Kastner, T., Plutzar, C., Bais, A. L. S., Carvalhais, N., Fetzel, T., Gingrich, S., Haberl, H., Lauk, C., Niedertscheider, M., Pongratz, J., Thurner, M., & Luyssaert, S. (2018). Unexpectedly large impact of forest management and grazing on global vegetation biomass. *Nature*, *553*(7686), 73–76. https://doi.org/10.1038/nature25138

Fang, J. Y., Yu, G. R., Liu, L. L., Hu, S. J., & Chapin, F. S. (2018). Climate change, human impacts, and carbon sequestration in China. *Proceedings of the National Academy of Sciences*, *115*(16), 4015–4020. https://doi.org/10.1073/pnas.1700304115

Fang, K., Qin, S. Q., Chen, L. Y., Zhang, Q. W., & Yang, Y. H. (2019). Al/Fe mineral controls on soil organic carbon stock across Tibetan alpine grasslands. *Journal of Geophysical Research. Biogeosciences*, *124*(2), 247–259. https://doi.org/10.1029/2018JG004782

Farmer, V. C., Delbos, E., & Miller, J. D. (2005). The role of phytolith formation and dissolution in controlling concentrations of silica in soil solutions and streams. *Geoderma*, *127*(1–2), 71–79. https://doi.org/10.1016/j.geoderma.2004.11.014

Fay, P. A., Prober, S. M., Harpole, W. S., Knops, J. M. H., Bakker, J. D., Borer, E. T., Lind, E. M., MacDougall, A. S., Seabloom, E. W., Wragg, P. D., Adler, P. B., Blumenthal, D. M., Buckley, Y. M., Chu, C., Cleland, E. E., Collins, S. L., Davies, K. F., Du, G., Feng, X., … Yang, L. H. (2015). Grassland productivity limited by multiple nutrients. *Nature Plants*, *1*(7), 15080. https://doi.org/10.1038/nplants.2015.80

Fishkis, O., Ingwersen, J., & Streck, T. (2009). Phytolith transport in sandy sediment: Experiments and modeling. *Geoderma*, *151*(3), 168–178. https://doi.org/10.1016/j.geoderma.2009.04.003

Fraysse, F., Pokrovsky, O. S., Schott, J., & Meunier, J. D. (2006). Surface properties, solubility and dissolution kinetics of bamboo phytoliths. *Geochimica Et Cosmochimica Acta*, *70*(8), 1939–1951. https://doi.org/10.1016/j.gca.2005.12.025

Gherardi, L. A., & Sala, O. E. (2020). Global patterns and climatic controls of belowground net carbon fixation. *Proceedings of the National Academy of Sciences*, *117*(33), 20038–20043. https://doi.org/10.1073/pnas.2006715117

Guo, F. S., Song, Z. L., Sullivan, L., Wang, H. L., Liu, X. Y., Wang, X. D., Li, Z. M., & Zhao, Y. Y. (2015). Enhancing phytolith carbon sequestration in rice ecosystems through basalt powder amendment. *Science Bulletin*, *60*(6), 591–597. https://doi.org/10.1007/s11434-015-0729-8

Hanssen, S. V., Daioglou, V., Steinmann, Z. J. N., Doelman, J. C., Van Vuuren, D. P., & Huijbregts, M. A. J. (2020). The climate change mitigation potential of bioenergy with carbon capture and storage. *Nature Climate Change*, *10*, 1023–1029. https://doi.org/10.1038/s41558-020-0885-y

Hodson, M. J. (2016). The development of phytoliths in plants and its influence on their chemistry and isotopic composition. Implications for palaeoecology and archaeology. *Journal of Archaeological Science*, *68*, 62–69. https://doi.org/10.1016/j.jas.2015.09.002

Hodson, M. J., White, P. J., Mead, A., & Broadley, M. R. (2005). Phylogenetic variation in the silicon composition of plants. *Annals of Botany*, *96*(6), 1027–1046. https://doi.org/10.1093/aob/mci255

Hu, Z. M., Fan, J. W., Zhong, H. P., & Yu, G. R. (2006). Spatiotemporal dynamics of aboveground primary productivity along a precipitation gradient in Chinese temperate grassland. *Science in China*, *36*(12), 1154–1162. https://doi.org/10.3969/j.issn.1674-7240.2006.12.010

Ji, Z., Yang, X. M., Song, Z. L., Liu, H. Y., Liu, X., Qiu, S., Li, J. W., Guo, F. S., Wu, Y. T., & Zhang, X. D. (2018). Silicon distribution in meadow steppe and typical steppe of northern China and its implications for phytolith carbon sequestration. *Grass and Forage Science*, *73*(2), 482–492. https://doi.org/10.1111/gfs.12316

Jiang, G. M., Han, X. G., & Wu, J. G. (2006). Restoration and management of the inner mongolia grassland require a sustainable strategy. *AMBIO: A Journal of the Human Environment*, *35*(5), 269–270. https://doi.org/10.1579/06-S-158.1

Jin, D. M., Ma, J. J., Ma, W. H., Liang, C. Z., Shi, Y., & He, J. S. (2013). Legumes in Chinese natural grasslands: Species, biomass, and distribution. *Rangeland Ecology & Management*, *66*(6), 648–656. https://doi.org/10.2111/REM-D-12-00159.1

Jin, D. Y., Murray, P. J., Xin, X. P., Qin, Y. F., Chen, B. R., Qing, G. L., Zhang, Z., & Yan, R. R. (2018). Attribution of explanatory factors for change in soil organic carbon density in the native grasslands of Inner Mongolia, China. *Journal of Arid Land*, *10*(3), 375–387. https://doi.org/10.1007/s40333-018-0056-4

Kawamura, K., Akiyama, T., Yokota, H., Tsutsumi, M., Yasuda, T., Watanabe, O., & Wang, S. (2005). Quantifying grazing intensities using geographic information systems and satellite remote sensing in the Xilingol steppe region, Inner Mongolia, China. *Agriculture, Ecosystems & Environment*, *107*(1), 83–93. https://doi.org/10.1016/j.agee.2004.09.008

Li, Z. M., De Tombeur, F., Linden, C. V., Cornelis, J. T., & Delvaux, B. (2020). Soil microaggregates store phytoliths in a sandy loam. *Geoderma*, *360*, 114037. https://doi.org/10.1016/j.geoderma.2019.114037

Li, Z. M., Song, Z. L., & Cornelis, J. T. (2014). Impact of rice cultivar and organ on elemental composition of phytoliths and the release of bio-available silicon. *Frontiers in Plant Science*, *5*(529), 1–8. https://doi.org/10.3389/fpls.2014.00529

Li, Z. M., Song, Z. L., & Li, B. L. (2013). The production and accumulation of phytolith-occluded carbon in Baiyangdian reed wetland of China. *Applied Geochemistry*, *37*, 117–124. https://doi.org/10.1016/j.apgeochem.2013.07.012

Li, Z. M., Unzuebelmonte, D., Cornelis, J. T., Linden, C. V., Struyf, E., Ronsse, F., & Delvaux, B. (2019). Effects of phytolithic rice-straw biochar, soil buffering capacity and pH on silicon bioavailability. *Plant and Soil*, *438*(1), 187–203. https://doi.org/10.1007/s11104-019-04013-0

Liu, H. Y., Mi, Z. R., Lin, L., Wang, Y. H., Zhang, Z. H., Zhang, F. W., Wang, H., Liu, L. L., Zhu, B., Cao, G. M., Zhao, X. Q., Sanders, N. J., Classen, A. T., Reich, P. B., & He, J. S. (2018a). Shifting plant species composition in response to climate change stabilizes grassland primary production. *Proceedings of the National Academy of Sciences*, *115*(16), 4051–4056. https://doi.org/10.1073/pnas.1700299114

Liu, S. S., Yang, Y. H., Shen, H. H., Hu, H. F., Zhao, X., Li, H., Liu, T. X., & Fang, J. Y. (2018b). No significant changes in topsoil carbon in the grasslands of northern China between the 1980s and 2000s. *Science of the Total Environment*, *624*, 1478–1487. https://doi.org/10.1016/j.scitotenv.2017.12.254

Lu, F., Hu, H., Sun, W., Zhu, J., Liu, G., Zhou, W., Zhang, Q., Shi, P., Liu, X., Wu, X., Zhang, L. U., Wei, X., Dai, L., Zhang, K., Sun, Y., Xue, S., Zhang, W., Xiong, D., Deng, L., … Yu, G. (2018). Effects of national ecological restoration projects on carbon sequestration in China from 2001 to 2010. *Proceedings of the National Academy of Sciences*, *115*(16), 4039–4044. https://doi.org/10.1073/pnas.1700294115

Luo, Z. K., Wang, G. C., & Wang, E. L. (2019). Global subsoil organic carbon turnover times dominantly controlled by soil properties rather than climate. *Nature Communications*, *10*(1), 1–10. https://doi.org/10.1038/s41467-019-11597-9

Ma, J. F. (2003). Functions of silicon in higher plants, silicon biomineralization. *Springer*, 127–147. https://doi.org/10.1007/978-3-642-55486-5_5

Ma, W. H., Fang, J. Y., Yang, Y. H., & Mohammat, A. (2010). Biomass carbon stocks and their changes in northern China's grasslands during 1982–2006. *Science China Life Sciences*, *53*(7), 841–850. http://doi.org/10.1007/s11427-010-4020-6

Ma, J. J., Ji, C. J., Han, M., Zhang, T. F., Yan, X. D., Hu, D., Zeng, H., & He, J. S. (2012). Comparative analyses of leaf anatomy of dicotyledonous species in Tibetan and Inner Mongolian grasslands. *Science China Life Sciences*, *55*(001), 68–79. https://doi.org/10.1007/s11427-012-4268-0

Meena, V. D., Dotaniya, M. L., Coumar, V., Rajendiran, S., Ajay, S., Kundu, S., & Subba Rao, A. (2014). A case for silicon fertilization to improve crop yields in tropical soils. *Proceedings of the National Academy of Sciences India*, *84*(3), 505–518. https://doi.org/10.1007/s40011-013-0270-y

Meunier, J. D., & Fabrice, C. (1999). Biogenic silica storage in soils. *Geology*, *27*(9), 835–838.

Mu, C., Zhang, T., Wu, Q., Peng, X., Cao, B., Zhang, X., Cao, B., & Cheng, G. (2015). Editorial: Organic carbon pools in permafrost regions on the Qinghai-Xizang (Tibetan) Plateau. *The Cryosphere*, *9*(2), 479–486. https://doi.org/10.5194/tc-9-479-2015

Neumann, D. (2003). *Silicon in plants*, *silicon biomineralization* (pp. 149–160). Springer. https://doi.org/10.1007/978-3-642-55486-5_6

Nguyen, M. N., Dultz, S., & Guggenberger, G. (2014). Effects of pretreatment and solution chemistry on solubility of rice-straw phytoliths.

Journal of Plant Nutrition and Soil Science, 177(3), 349–359. https://doi.org/10.1002/jpln.201300056

Nguyen, M. N., Dultz, S., Meharg, A., Pham, Q. V., Hoang, A. N., Dam, T. T. N., Nguyen, V. T., Nguyen, K. M., Nguyen, H. X., & Nguyen, N. T. (2019). Phytolith content in Vietnamese paddy soils in relation to soil properties. *Geoderma*, *333*, 200–213. https://doi.org/10.1016/j.geoderma.2018.07.027

Pan, W., Song, Z., Liu, H., Müeller, K., Yang, X., Zhang, X., Li, Z., Liu, X. U., Qiu, S., Hao, Q., & Wang, H. (2017). Impact of grassland degradation on soil phytolith carbon sequestration in Inner Mongolian steppe of China. *Geoderma*, *308*, 86–92. https://doi.org/10.1016/j.geoderma.2017.08.037

Parr, J. F., & Sullivan, L. A. (2005). Soil carbon sequestration in phytoliths. *Soil Biology & Biochemistry*, *37*(1), 117–124. https://doi.org/10.1016/j.soilbio.2004.06.013

Parr, J. F., & Sullivan, L. A. (2014). Comparison of two methods for the isolation of phytolith occluded carbon from plant material. *Plant and Soil*, *374*, 45–53. https://doi.org/10.1007/s11104-013-1847-1

Parr, J. F., Sullivan, L. A., Chen, B. H., Ye, G. F., & Zheng, W. P. (2010). Carbon bio-sequestration within the phytoliths of economic bamboo species. *Global Change Biology*, *16*(10), 2661–2667. https://doi.org/10.1111/j.1365-2486.2009.02118.x

Piperno, D. R. (1988). Phytolith analysis. *An Archaeological and Geological Perspective*, *280*. https://doi.org/10.1002/gea.3340050207

Qi, L. M., Li, Y. H., Huang, Z. T., Jiang, P. K., Baoyin, T. G. T., & Wang, H. L. (2016). Phytolith-occluded organic carbon as a mechanism for long-term carbon sequestration in a typical steppe: The predominant role of belowground productivity. *Science of the Total Environment*, *577*, 413–417. https://doi.org/10.1016/j.scitotenv.2016.10.206

Schimel, D. S., Braswell, B. H., Holland, E. A., Mckeown, R., Ojima, D. S., Painter, T. H., Parton, W. J., & Townsend, A. R. (1994). Climatic, edaphic, and biotic controls over storage and turnover of carbon in soils. *Global Biogeochemical Cycles*, *8*(3), 279–293. https://doi.org/10.1029/94GB00993

Schuur, E. A. G., McGuire, A. D., Schädel, C., Grosse, G., Harden, J. W., Hayes, D. J., Hugelius, G., Koven, C. D., Kuhry, P., Lawrence, D. M., Natali, S. M., Olefeldt, D., Romanovsky, V. E., Schaefer, K., Turetsky, M. R., Treat, C. C., & Vonk, J. E. (2015). Climate change and the permafrost carbon feedback. *Nature*, *520*(7546), 171–179. https://doi.org/10.1038/nature14338

Seyfferth, A. L., Kocar, B. D., Lee, J. A., & Fendorf, S. (2013). Seasonal dynamics of dissolved silicon in a rice cropping system after straw incorporation. *Geochimica Et Cosmochimica Acta*, *123*(1), 120–133. https://doi.org/10.1016/j.gca.2013.09.015

Shen, H. H., Zhu, Y. K., Zhao, X., Geng, X. Q., & Fang, J. Y. (2016). Analysis of current grassland resources in China. *Chinese Science Bulletin*, *61*(2), 139. https://doi.org/10.1360/N972015-00732

Shimono, A., Zhou, H. K., Shen, H. H., Hirota, M., Ohtsuka, T., & Tang, Y. H. (2010). Patterns of plant diversity at high altitudes on the Qinghai-Tibetan Plateau. *Journal of Plant Ecology*, *3*(1), 1–7. https://doi.org/10.1093/jpe/rtq002

Song, Z. L., Liu, H. Y., Si, Y., & Yin, Y. (2012b). The production of phytoliths in China's grasslands: Implications to the biogeochemical sequestration of atmospheric CO_2. *Global Change Biology*, *18*(12), 3647–3653. https://doi.org/10.1111/gcb.12017

Song, Z. L., Mcgrouther, K., & Wang, H. L. (2016). Occurrence, turnover and carbon sequestration potential of phytoliths in terrestrial ecosystems. *Earth-Science Reviews*, *158*, 19–30. https://doi.org/10.1016/j.earscirev.2016.04.007

Song, Z. L., Wang, H. L., Strong, P. J., Li, Z. M., & Jiang, P. K. (2012a). Plant impact on the coupled terrestrial biogeochemical cycles of silicon and carbon: Implications for biogeochemical carbon sequestration. *Earth-Science Reviews*, *115*(4), 319–331. https://doi.org/10.1016/j.earscirev.2012.09.006

Tang, X., Zhao, X., Bai, Y., Tang, Z., Wang, W., Zhao, Y., Wan, H., Xie, Z., Shi, X., Wu, B., Wang, G., Yan, J., Ma, K., Du, S., Li, S., Han, S., Ma, Y., Hu, H., He, N., … Zhou, G. (2018). Carbon pools in China's terrestrial ecosystems: New estimates based on an intensive field survey. *Proceedings of the National Academy of Sciences*, *115*(16), 4021–4026. https://doi.org/10.1073/pnas.1700291115

Tang, Z., Fang, J., Chi, X., Yang, Y., Ma, W., Mohhamot, A., Guo, Z., Liu, Y., & Gaston, K. J. (2012). Geography, environment, and spatial turnover of species in China's grasslands. *Ecography*, *35*(12), 1103–1109. https://doi.org/10.1111/j.1600-0587.2012.07713.x

Tombeur, F. D., Laliberté, E., Lambers, H., Faucon, M. P., Zemunik, G., Turner, B. L., Cornelis, J. T., & Mahy, G. (2021). A shift from phenol to silica-based leaf defences during long-term soil and ecosystem development. *Ecology Letters*, *24*(5), 984–995. https://doi.org/10.1111/ele.13713

Torn, M. S., Trumbore, S. E., Chadwick, O. A., Vitousek, P. M., & Hendricks, D. M. (1997). Mineral control of soil organic carbon storage and turnover. *Nature*, *389*(6647), 170–173. https://doi.org/10.1038/38260

Walkley, A., & Black, I. A. (1934). An examination of the degtjareff method for determining soil organic matter, and a proposed modification of the chromic acid titration method. *Soil Science*, *37*(1), 29–38. https://doi.org/10.1097/00010694-193401000-00003

Wiesmeier, M., Munro, S., Barthold, F., Steffens, M., Schad, P., & Kogelknabner, I. (2015). Carbon storage capacity of semi-arid grassland soils and sequestration potentials in northern China. *Global Change Biology*, *21*(10), 3836–3845. https://doi.org/10.1111/gcb.12957

Wilding, L. P. (1967). Radiocarbon dating of biogenetic opal. *Science*, *156*(156), 66–67. https://doi.org/10.1126/science.156.3771.66

Wilding, L. P., Brown, R. E., & Holowaychuk, N. (1967). Accessibility and properties of occluded carbon in biogenetic opal. *Soil Science*, *103*(1), 56–61. https://doi.org/10.1097/00010694-196701000-00009

Wynn, J. G., Bird, M. I., Vellen, L., Grandclement, E., Carter, J., & Berry, S. L. (2006). Continental-scale measurement of the soil organic carbon pool with climatic, edaphic, and biotic controls. *Global Biogeochemical Cycles*, *20*(1). https://doi.org/10.1029/2005GB002576

Yan, Y. E., Zhou, X. H., Jiang, L. F., & Luo, Y. Q. (2017). Effects of carbon turnover time on terrestrial ecosystem carbon storage. *Biogeosciences*, *14*(23), 5441–5454. https://doi.org/10.5194/bg-14-5441-2017

Yang, Y. H., Fang, J. Y., Ji, C. J., Ma, W. H., Su, S. S., & Tang, Z. R. (2010). Soil inorganic carbon stock in the Tibetan alpine grasslands. *Global Biogeochemical Cycles*, *24*(4), 1–11. https://doi.org/10.1029/2010GB003804

Yang, Y. H., Fang, J. Y., Tang, Y. H., Ji, C. J., Zheng, C. Y., He, J. S., & Zhu, B. (2008). Storage, patterns and controls of soil organic carbon in the Tibetan grasslands. *Global Change Biology*, *14*(7), 1592–1599. https://doi.org/10.1111/j.1365-2486.2008.01591.x

Yang, Y. H., Mohammat, A., Feng, J. M., Zhou, R., & Fang, J. Y. (2007). Storage, patterns and environmental controls of soil organic carbon in China. *Biogeochemistry*, *84*(2), 131–141. https://doi.org/10.1007/s10533-007-9109-z

Yao, Y. T., Wang, X. H., Li, Y., Wang, T., Shen, M. G., Du, M. Y., He, H. L., Li, Y. N., Luo, W. J., Ma, M. G., Ma, Y. M., Tang, Y. H., Wang, H. M., Zhang, X. Z., Zhang, Y. P., Zhao, L., Zhou, G. S., & Piao, S. L. (2018). Spatiotemporal pattern of gross primary productivity and its covariation with climate in China over the last thirty years. *Global Change Biology*, *24*(1), 184–196. https://doi.org/10.1111/gcb.13830

Zhang, X. D., Song, Z. L., Hao, Q., Yu, C. X., Liu, H. Y., Chen, C. M., Muller, K., & Wang, H. L. (2020). Storage of soil phytoliths and phytolith-occluded carbon along a precipitation gradient in grasslands of northern China. *Geoderma*, *364*, 114200. https://doi.org/10.1016/j.geoderma.2020.114200

Zhang, X. D., Song, Z. L., Mcgrouther, K., Li, J. W., Li, Z. M., Ru, N., & Wang, H. L. (2016a). The impact of different forest types on phytolith-occluded carbon accumulation in subtropical forest soils. *Journal of Soils & Sediments*, *16*(2), 461–466. https://doi.org/10.1007/s11368-015-1259-3

Zhang, X. S., Tang, H. P., Dong, X. B., Li, B., Huang, Y. M., & Guo, J. R. (2016b). The dilemma of steppe and it's transformationin China. *Chinese Science Bulletin*, *61*(2), 165. https://doi.org/10.1360/N972015-00738

Zhao, Y. Y., Song, Z. L., Xu, X. T., Liu, H. Y., Wu, X. C., Li, Z. M., Guo, F. S., & Pan, W. J. (2015). Nitrogen application increases phytolith carbon sequestration in degraded grasslands of North China. *Ecological Research*, *31*, 117–123. https://doi.org/10.1007/s11284-015-1320-0

Zuo, X. X., Lu, H. Y., & Gu, Z. Y. (2014). Distribution of soil phytolith-occluded carbon in the Chinese Loess Plateau and its implications for silica–carbon cycles. *Plant and Soil*, *374*(1–2), 223–232. https://doi.org/10.1007/s11104-013-1850-6

How to cite this article: Song, Z., Wu, Y., Yang, Y., Zhang, X., Van Zwieten, L., Bolan, N., Li, Z., Liu, H., Hao, Q., Yu, C., Sun, X., Song, A., Wang, W., Liu, C., & Wang, H. (2022). High potential of stable carbon sequestration in phytoliths of China's grasslands. *Global Change Biology*, 00, 1–15. https://doi.org/10.1111/gcb.16092